

# Engineering Notes

ENGINEERING NOTES are short manuscripts describing new developments or important results of a preliminary nature. These Notes cannot exceed 6 manuscript pages and 3 figures; a page of text may be substituted for a figure and vice versa. After informal review by the editors, they may be published within a few months of the date of receipt. Style requirements are the same as for regular contributions (see inside back cover).

## A80-049 Symmetric Body Vortices on Slender Bodies of Revolution at Transonic Speeds

J.R. Deane\* and M.H. Ponting†

British Aerospace Dynamic Group, Bristol, England  
and

K.A. Fellows‡

Aircraft Research Association, Bedford, England

### Introduction

RECENT interest in high angle of incidence flight for missiles has prompted much experimental and theoretical work into the phenomena of body vortex generation. A key feature which emphasizes the requirement for accurate knowledge of body vortex characteristics is the need for the calculation of the load on a wing panel rolled into the leeside of a body at an angle of incidence to the oncoming flow. Without an accurate estimate of the body vortex position and strength it would be virtually impossible to obtain reliable values of panel load and hence to predict induced rolling moments on missile-type shapes. Recent work by Oberkampf<sup>1</sup> has stressed this point.

Although much effort is currently directed toward the asymmetric body vortex problem at high angles of incidence, work is still required to adequately resolve questions relating to phenomena at lower angles of incidence.

Experimental studies of body vortex characteristics are necessary to enhance the data base by which theoretical and semiempirical methods may be tested or, from which, totally empirical techniques may be developed. The latter are most appropriate to those situations where reasonable accuracy is required coupled with economy.

In an example of the empirical representation of body vortex characteristics, Mendenhall and Nielsen<sup>2</sup> compiled the results available to them, but the data coverage was neither extensive nor systematic. Results from vastly different test conditions were included. Data for incompressible and supersonic speeds, hemispherical noses, and sharp cones were correlated together in an attempt to form an understanding of the important parameters. There was a notable lack of information in the middle of the speed range for high subsonic, transonic, and low supersonic Mach numbers. The forms of correlation adopted therefore can only be described as tentative. Wardlaw<sup>3</sup> in his more recent survey paper included extra information but, again, data coverage has been mainly in the near incompressible or reasonably high supersonic speed regimes.

A particular need has thus been identified for further information concerning the characteristics of symmetric body vortices at transonic speeds.

### Test Description

A series of experiments has been undertaken to supplement available information on body vortex characteristics. The tests, which were conducted in the  $2.74 \times 2.44$  m transonic wind tunnel at the Aircraft Research Association, were performed on two bodies of revolution at moderate angles of incidence in transonic flow. Each model consisted of a cylindrical section and boat-tail to which two alternative nose shapes could be fitted (tangent ogive or ellipsoidal of fineness ratios 1.215 and 1.00, respectively; see Fig. 1). The models were mounted on a conventional straight sting support of diameter  $0.38D$  attached to the quadrant and were pitched to angles of incidence ( $\sigma$ ) of 8.1, 15.1, and 20.7 deg. The freestream Mach numbers ( $M$ ) for the tests were 0.7 and 1.15 and the Reynolds numbers, based on body diameter, were  $1.46$  and  $1.70 \times 10^6$ , respectively. The freestream turbulence level expressed as a noise level  $C_{p_{rms}}$  was approximately 2.5% at  $M=0.7$  and 0.75% at  $M=1.15$ .

Flowfield information was gathered in the leeside wake of the bodies by the use of a rake of 16 five-hole yawmeter

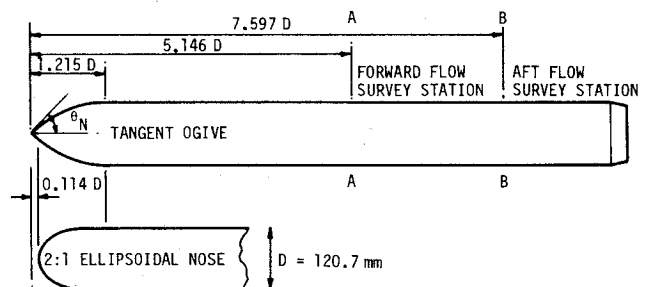


Fig. 1 General arrangement of model.

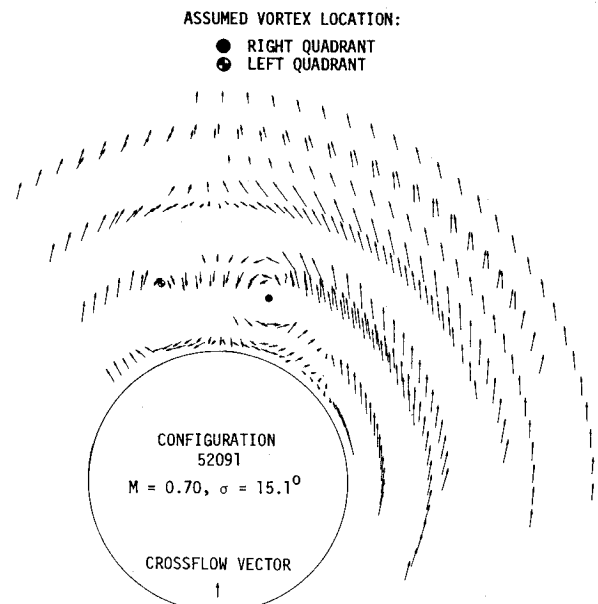


Fig. 2 Flow vectors in leeside wake.

Received Aug. 14, 1979; revision received Jan. 21, 1980. Copyright © American Institute of Aeronautics and Astronautics, Inc., 1980. All rights reserved.

Index categories: LV/M Aerodynamics; Transonic Flow; Jets, Wakes, and Viscid-Inviscid Flow Interactions.

\*Section Leader, Aerodynamics Research Department. Member AIAA.

†Research Engineer, Theoretical Studies Department, (now at Royal Military College of Science, Shrivenham).

‡Project Supervisor.

Table 1 Test notation and flow conditions

Configuration	Nose shape	Rake position	Mach number	Incidence $\sigma$ , deg
52061	Ogive	Forward	0.7 and 1.15	8.1, 15.1, 20.7
52071	Ellipsoidal	Forward	0.7	8.1, 15.1, 20.7
52081	Ellipsoidal	Aft	0.7	8.1, 15.1, 20.7
52081	Ellipsoidal	Aft	1.15	8.1, 15.1, 20.7
52091	Ogive	Aft	0.7	8.1, 15.1, 20.7
52091	Ogive	Aft	1.15	8.1, 15.1, 20.7

Table 2 Summary of test results

Configuration	$M$	$\sigma$	Core location <sup>a</sup>		$\frac{\Gamma_t}{\pi DV_\infty \sin \sigma}$	$\Gamma_s/\Gamma_t$
			$y/D$	$z/D$		
52061	0.7	8.1	...	...	0.164	...
		15.1	0.22	0.65	0.370	0.23
		20.7	0.22	0.67	0.468	0.30
52061	1.15	8.1	...	...	0.232	...
		15.1	0.28	0.61	0.429	0.39
		20.7	0.37	0.75	0.659	0.45
52071	0.7	8.1	...	...	0.185	...
		15.1	0.23	0.62	0.390	0.21
		20.7	0.21	0.68	0.473	0.30
52081	0.7	8.1	0.19	0.66	0.371	0.28
		15.1	0.21	0.75	0.610	0.22
		20.7	0.23	0.82	0.775	0.26
52081	1.15	8.1	0.25	0.60	0.346	0.35
		15.1	0.23	0.79	0.686	0.25
		20.7	0.30	1.04	1.031	0.25
52091	0.7	8.1	...	...	0.327	...
		15.1	0.19	0.71	0.593	0.32
		20.7	0.21	0.78	0.748	0.27
52091	1.15	8.1	0.23	0.61	0.366	0.33
		15.1	0.24	0.78	0.699	0.21
		20.7	0.29	1.03	0.938	0.35

<sup>a</sup> Lateral and vertical locations perpendicular to body longitudinal axis.

probes. The body and the attached yawmeter rake were rolled together around the body axis to yield velocity vectors in two crossflow planes AA and BB, shown on Fig. 1, at a maximum of 400 points in each survey plane.

### Results

Although the data does exhibit a nonuniform coverage of the field, flow survey information is available from which the vortex positions and strengths can be determined.

#### Vortex Core Locations and Strengths

From flow vector plots (e.g., Fig. 2) vortex core locations can be deduced subjectively by observing where the most rapid changes in crossflow velocity vectors occur and where the magnitude of those vectors decreases to a minimum. Here it is assumed that a viscous representation is appropriate, yielding low induced velocities as the core is approached.

Circuit integrations can also be performed to calculate the circulation enclosed in any given segment of the flowfield. Figure 3 illustrates the segments chosen for the same experimental case as was shown in Fig. 2. Note that the size of some segments is large, reflecting a lack of detailed data in various portions of the leeside area.

From the various sets of experimental data, vortex core locations have been deduced and also circuit integrations performed to give the total circulation present in an area

bounded by the outermost circumferential traverse lines in the leeside quadrant. The latter procedure will yield a value of circulation ( $\Gamma_t$ ) or vortex strength which can be compared with values derived in other tests and incorporated in the empirical methods. Test results are summarized in Tables 1 and 2. A dash in Table 2 indicates where it was impossible to deduce a vortex position owing to scarcity of flow data in the appropriate area.

Since the circuit integration paths have natural limits set by the outermost circumferential traverse line, it is probable that a proportion of the circulation present in the leeside flowfield has not been included. However, it is anticipated that little accuracy has been lost since it was observed that the contributions to the net circulation of the outermost flowfield segments were becoming relatively small.

The following general trends are found in the data. For nondimensionalized vortex strength the supersonic speed data are greater in magnitude than those for subsonic speeds and, for position, further outboard in the lateral sense. The effect of Mach number on vertical vortex coordinate is relatively smaller than the effect on lateral coordinate.

#### Vortex Feeding Sheets

Current simple prediction methods use single line vortex representations for the estimation of interference terms and thus it is relevant to be able to assess, from the available

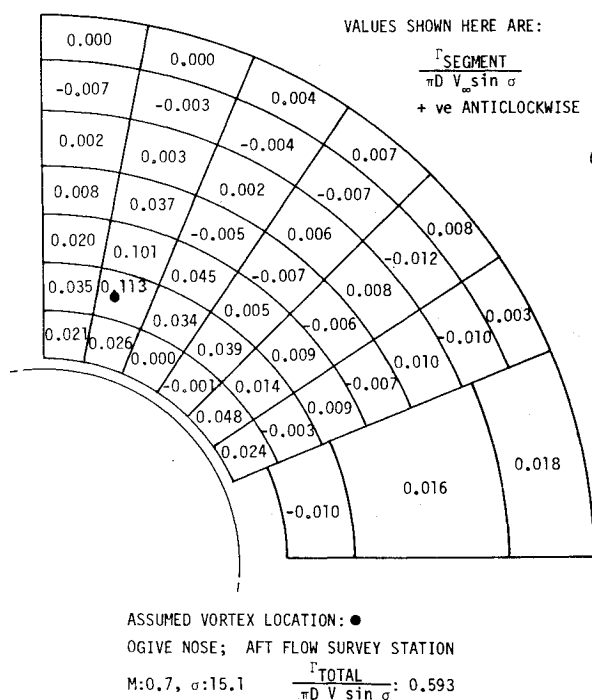


Fig. 3 Distribution of circulation within leeside wake.

information, the relative importance of core and feeding sheet in the leeside quadrant.

Circuit integrations for the ogive nose at  $M=1.15$  and  $\sigma=15.1$  and  $20.7$  deg have shown that the vortex feeding sheet can contain 21-35% of the circulation in the leeside area under these conditions for the aft flow survey location. This percentage may be compared with values of 40-60% from tests<sup>1</sup> at higher supersonic Mach numbers. Other results are given in Table 2. Most of the data for  $\Gamma_s/\Gamma_t$  lie in the range 0.21-0.35. (Subscripts  $s$  and  $t$  refer to sheet and total values.) The values are more reliable for the aft flow survey location since at that point the development of the flow pattern into a core and feeding sheet was more easily observed. Changes in flow condition are seen to have little systematic effect on the ratio  $\Gamma_s/\Gamma_t$ .

### Concluding Remarks

As part of an effort to improve prediction methods for the aerodynamic characteristics of missiles, flow survey tests have been performed which contribute some new information on the characteristics of symmetric body vortex systems at transonic speeds. The test program has included experiments on a tangent ogive forebody with a high nose semiapex angle and also a body with an ellipsoidal nose.

Values of vortex strength, and vertical and lateral location have been deduced from the velocity vector information obtained in the leeside wake of the body. The relative importance of the feeding sheet and vortex core has been assessed. It was found that the former can contain 21-35% of the circulation in the leeside quadrant.

### References

- <sup>1</sup>Oberkampf, W.L., "Prediction of Forces and Moments on Finned Missiles in Subsonic Flow," AIAA Paper 79-0365, 17th Aerospace Sciences Meeting, New Orleans, La., Jan. 1979.
- <sup>2</sup>Mendenhall, M.R. and Nielsen J.N., "Effect of Symmetrical Vortex Shedding on the Longitudinal Aerodynamic Characteristics of Wing-Body-Tail Combinations," NASA CR-2473, Jan. 1975.
- <sup>3</sup>Wardlaw, A.B., "High Angle of Attack Missile Aerodynamics," AGARD-LS-98, March 1979.

## A80-050 Ignition Delay Studies on Hybrid Propellant Grains

K. Pitchaiah\* and P.M.M. Krishna†  
Indian Institute of Science, Bangalore, India

### Introduction

IN hybrid rockets, the propellant grain consists of a mixture of ground solid fuel, finely divided metal powder, fractional percents of additives used for increasing the burn rate, and a polymer as binder. In the past, several hypergolic hybrid fuels associated with nitric acid have been developed and their ignition delays measured as a function of physical and chemical factors.<sup>1-4</sup> However, not much effort was given to the simulation of actual rocket conditions by embedding the hypergolic solid fuels in a binder and measuring the ignition delays. Recently, solid amines<sup>5</sup> have been used with various binders in hypergolic hybrid propellant grains. The hypergolic combustion of propellant grain containing a mixture of tetraformal trisazine and OH-terminated polybutadiene with  $\text{HNO}_3$  has recently been reported.<sup>6</sup> The use of several other fuels and binders has been reported in the literature.<sup>7-9</sup>

In the present investigation, the ignition delays of some of the hydrazones embedded in a polymer matrix have been measured as a function of: 1) weight of the propellant grain, 2) polymer binder type, 3) polymer binder loading, and 4) metal loading.

### Experimental

#### Materials

Furfuraldehyde phenylhydrazine (FPH) was prepared following the procedure described earlier.<sup>2</sup> Formaldehyde phenylhydrazine polymer (FORPH) was prepared by reacting phenylhydrazine with a little excess of formaldehyde solution. The yellow solid mass (polymer type) was separated from the beaker, washed with an alcohol-water mixture and dried in vacuum. Commercially available phenolformaldehyde (PF) was used in the present study. The nitric acid having 91%  $\text{HNO}_3$ , 7%  $\text{NO}_2$ , and 2%  $\text{H}_2\text{O}$  by weight was used in all experiments.

#### Propellant Grains

The polymeric binder, formaldehyde phenylhydrazine or phenolformaldehyde, was melted and mixed with fuel powders until a homogeneous mixture resulted. The mixture was then transferred into a test tube and allowed to solidify at  $5^\circ\text{C}$  for three days. The cured propellant grains were cut to size and used in the form of a tablet for measuring ignition delays (ID). The grains are easily processed and have good physical properties. All ID's were measured by using the setup described in Ref. 4.

### Results and Discussion

The experimental results showing the minimum ignition delays for furfuraldehyde phenylhydrazine and benzaldehyde phenylhydrazine taken in the polymer matrix are given in Table 1. The FPH/FORPH- $\text{HNO}_3$  system gave the least ID at 300 mg weight of the propellant grain using 0.55 ml of nitric acid.

Received Aug. 10, 1979; revision received Nov. 28, 1979. Copyright © American Institute of Aeronautics and Astronautics, Inc., 1980. All rights reserved.

Index categories: Fuels and Propellants, Properties of; Solid and Hybrid Rocket Engines: Combustion Stability, Ignition, and Detonation.

\*Project Assistant, Dept. of Inorganic and Physical Chemistry.

†Presently, Research Associate Dept. of Chemistry, Wright State University, Dayton, Ohio.